

9-26-1995

Dental Abnormalities and Early Diagnosis of Hyperphosphatasemia

M. J. Bottero-Cornillac
Aix-Marseille Université

A. Gaucher
Université de Lorraine

C. Wang
Université de Lorraine

M. Chaussidon
LP 6709 CNRS

J. Yvon
URA 235 CNRS

Follow this and additional works at: <https://digitalcommons.usu.edu/microscopy>

 Part of the [Biology Commons](#)

Recommended Citation

Bottero-Cornillac, M. J.; Gaucher, A.; Wang, C.; Chaussidon, M.; and Yvon, J. (1995) "Dental Abnormalities and Early Diagnosis of Hyperphosphatasemia," *Scanning Microscopy*: Vol. 9 : No. 4 , Article 20.

Available at: <https://digitalcommons.usu.edu/microscopy/vol9/iss4/20>

This Article is brought to you for free and open access by the Western Dairy Center at DigitalCommons@USU. It has been accepted for inclusion in Scanning Microscopy by an authorized administrator of DigitalCommons@USU. For more information, please contact digitalcommons@usu.edu.



DENTAL ABNORMALITIES AND EARLY DIAGNOSIS OF HYPERPHOSPHATASEMIA

M.J. Bottero-Cornillac^{1,4,*}, A. Gaucher², C. Wang², M. Chaussidon³ and J. Yvon⁴

¹IMEB EA 1787, UFR Odontologie, 13916 Marseille, ²URA 1288 CNRS, UFR Médecine, 54501 Vandoeuvre, ³LP 6709 CNRS, 54501 Vandoeuvre, ⁴URA 235 CNRS, LEM, 54501 Vandoeuvre, France

(Received for publication June 23, 1994 and in revised form September 26, 1995)

Abstract

Introduction

Dental hard tissue abnormalities have never been described as part of the symptoms associated with hyperphosphatasemia. Fourteen teeth obtained from a young man, who had a mild form of hyperphosphatasemia, were analyzed using scanning electron microscopy (SEM), secondary ion mass spectroscopy (SIMS), X-ray diffraction (XRD), and infrared (IR) spectroscopy. SEM revealed a thin enamel, presenting a prismatic structure with many pits, and atypical cementum and dentin showing numerous resorption areas. The X-ray diffractograms revealed poorly crystalline hydroxyapatite associated with α -tricalcium phosphate and magnesium hydroxide phases. SIMS data showed high Ca concentrations: 40.5 weight % {wt%; standard deviation (SD) = 0.13} and 42.5 wt% (SD = 1.03) in enamel and dentin respectively, and high Ca/P weight ratios: 2.28 in the enamel, 2.65 in the dentin. The lack of crystallinity may be linked to the high content of proteins and magnesium adsorbed onto apatite.

This study demonstrates the need for thorough radiographical and biological investigations for skeletal abnormalities, even in the absence of systemic symptoms, when generalized dental abnormalities of both enamel and dentin are observed.

Key Words: Hyperphosphatasemia, enamel, dentin, cementum, calcium phosphates, magnesium hydroxide, scanning electron microscopy, secondary ion mass spectroscopy, infrared spectroscopy.

*Address for correspondence:

M.J. Bottero-Cornillac
IMEB EA 1787, Odontologie,
Faculté de Médecine secteur nord,
13916 Marseille Cedex 20,
France.

Telephone number: (33) 91 69 89 63
FAX number: (33) 91 69 89 64

The first report on hyperphosphatasemia (Bakwin and Eiger, 1956) described the case of a 7-year-old Puerto Rican girl. Only about 20 cases of hyperphosphatasemia have since been reported in the literature (Fanconi *et al.*, 1964; Stemmermann, 1966; Eyring and Eisenberg, 1968; Thompson *et al.*, 1969; Caffey, 1973; Whalen *et al.*, 1977; Iancu *et al.*, 1978; Dunn *et al.*, 1979; Döhler *et al.*, 1986; Nerlich *et al.*, 1992).

According to Caffey's (1973) definition, hyperphosphatasemia is an uncommon metabolic disease associated with high serum alkaline phosphatase, excessive excretion of hydroxyproline in the urine, and generalized skeletal disorders. Usually occurring during infancy, this anomaly is a polymorphic disorder. Within the same family, some patients can be clinically more affected than others (Bakwin *et al.*, 1964).

Teeth abnormalities have been rarely observed and described using scanning electron microscopy (SEM) and spectrographical methods. For either severe or mild forms of hyperphosphatasemia, only Eyring and Eisenberg (1968) have reported cases in which an opalescent discoloration and untimely loss of deciduous teeth were noted.

However, in mild forms of hyperphosphatasemia, dental abnormalities may be the first obvious manifestation of the disease. Since hyperphosphatasemia can be successfully treated with human thyrocalcitonin or disodium etidronate AHPD (amino hydroxypropidilene diphosphonate; Caffey, 1977; Spindler *et al.*, 1992), the identification of these dental disorders may allow early diagnosis and appropriate treatment of the disease.

The aim of this paper is to report structural and chemical modifications of permanent teeth obtained from a young man who had a mild form of undiagnosed hyperphosphatasemia.

Material and Methods

A 22-year-old man, with an uneventful health history except a complaint about back pain, was referred for apical surgery on the second right lower molar.

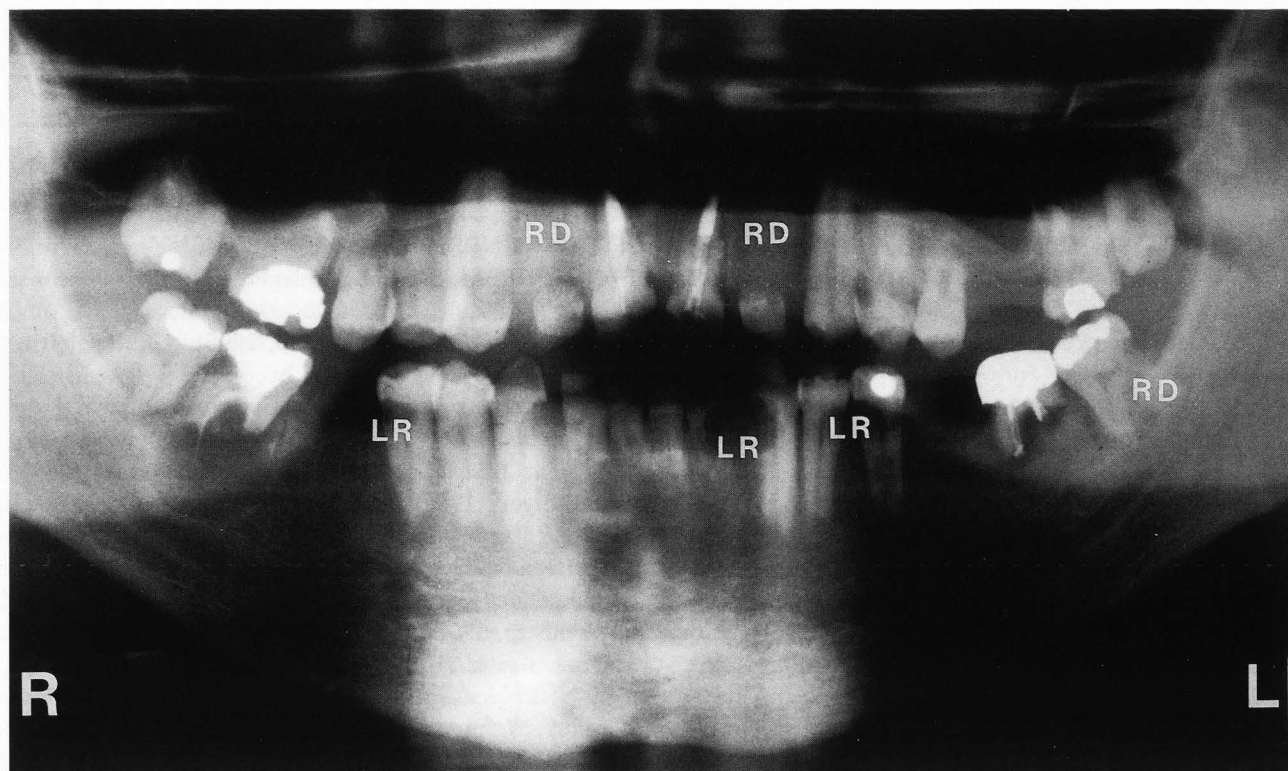


Figure 1. Panoramic radiograph. Note the linear resorption (LR) at the cervix level and the numerous root destructions (RD). A large periapical lesion associated with an important root resorption on the second right lower molar giving a pseudocystic aspect, was the motivation for the first consultation. R: right, L: left.

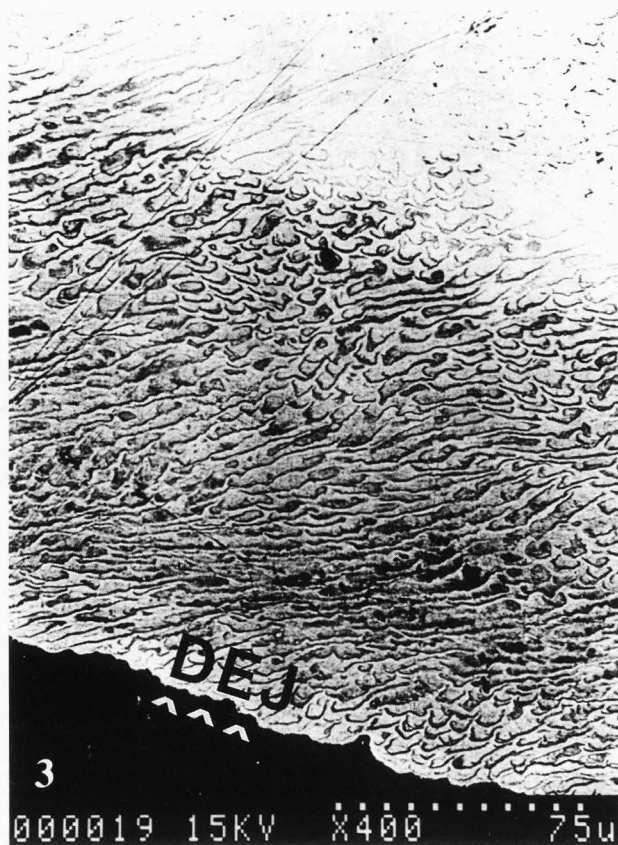
The first four lower and upper molars were missing. The other small-sized teeth were irregularly colored. Their yellowish brown enamel flaked off easily. Once enamel had flaked off, colored dentin did not show any decay. Hyperplastic gingiva crept into cervical erosions. An axial and transversal mobility was noted on every tooth, except on the left and right maxillary cuspids, the left and right mandibular cuspids, and the left and right mandibular bicuspid. A panoramic radiograph showed advanced root resorption and extensive periapical bone loss (Fig. 1).

Because the observed dental abnormalities were suspected to correspond to a systemic disease, the patient was referred to a physician. Clinical chemical analysis revealed a high serum alkaline phosphatase level: 904 mU/ml (well above the normal range of 70-260 mU/ml). A high level of hydroxyproline in the urine: (170 mg/24h instead of the normal 15-50 mg/24h) was also detected. Bone scintigraphy, using Tc-99m MDP (methylene di-phosphonate), showed a slightly increased activity of the whole skeleton. All these findings were consistent with hyperphosphatasemia.

Because of the mobility and the huge resorption destroying whole roots (Fig.1), the remnants of fourteen

permanent teeth, each of them with the same type of abnormalities, were harvested from this young man for prosthodontic reasons. All the extracted teeth affected, as well as 10 control teeth extracted for orthodontic reasons from healthy patients, were successively rinsed under tap water and in double-distilled water, cleaned by immersion in 10% sodium hypochlorite for 5 minutes to remove organic films only at the surface of teeth, thoroughly rinsed in double-distilled water for 1 hour and finally placed into an ultrasonic cleaner for 3 minutes (Kerebel and Daculsi, 1977). For SEM and secondary ion mass spectrometric (SIMS) investigations, 8 of the 14 teeth were randomly chosen, dehydrated in a graded ethanol series, and critical point dried using amyl acetate as an intermediate fluid.

Four of these 8 teeth were randomly selected (2 bicuspid and 2 molars), embedded in epoxy resin, and cut longitudinally with a diamond disk in a plane perpendicular to the buccal outer enamel surface. These were felt-polished to 0.4 μm with diamond paste, and sonicated in ethanol. The 4 other teeth (1 bicuspid and 3 incisors) were observed without any sectioning. The 8 teeth were sputter-coated with gold and examined in a Hitachi S-2500 SEM equipped with backscattered electron (BSE)



Figures 2 and 3. SEM examination of polished section of an affected tooth. **Figure 2.** The enamel thickness shows pathological variations between 450 and 1050 μm . Note the heterogeneous area in the inner first third of enamel near to the dentino-enamel junction (DEJ). Some cracks can be attributed to weakness lines (*) and others are artifacts. O: occlusal surface. Bar = 0.75 mm. **Figure 3.** When magnified, the enamel polished section revealed the porosity involving its inner first third (arrowhead) where prism sheath and interprismatic substance are enlarged. Bar = 75 μm .

imaging facilities.

The distribution of the chemical composition of the enamel and dentin was determined on the 4 gold sputtered sectioned teeth from the surface towards the dentino-enamel junction by SIMS. A Cameca IMS 3F spectrometer and conventional energy filtering techniques were used. The intensities of the $^1\text{H}^+$, $^{12}\text{C}^+$, $^{19}\text{F}^-$, $^{23}\text{Na}^+$, $^{24}\text{Mg}^+$, $^{31}\text{P}^+$, $^{39}\text{K}^+$, and $^{40}\text{Ca}^+$ peaks were measured. A standard apatite (Table 1; Roeder *et al.*, 1987), $\text{Ca}(\text{CO}_3)$ and $\text{Mg}(\text{OH})_2$ references were used to determine the emission yields of H, C, F, Na, Mg and Ca versus P. The results were converted to percent weight, assuming the sum of all elements to be 100%. The accuracy of the SIMS was 1%.

For Fourier-transform infrared (IR) spectroscopy (FTIRS) and X-ray diffraction (XRD) investigations, the last 6 of the 14 teeth were sliced and the enamel thoroughly separated from the dentin using a small chisel. Low magnification light microscopic observation was

Table 1. Chemical analysis of Durango apatite.

Durango apatite	weight percent
P	17.90
Ca	38.60
Ca/P	2.15
Na	0.05
F	3.50
Cl	0.30

Data from Roeder *et al.* (1987). Durango apatite was used as reference for SIMS analysis of affected enamel and dentin. This pure Mexican apatite has been associated with $\text{Mg}(\text{OH})_2$ and $\text{Ca}(\text{CO}_3)$ to provide a good standard for the SIMS.

performed to check that the enamel samples were free of dentin. Enamel and dentin samples were ground in an agate mortar to a particle size smaller than 40 μm .

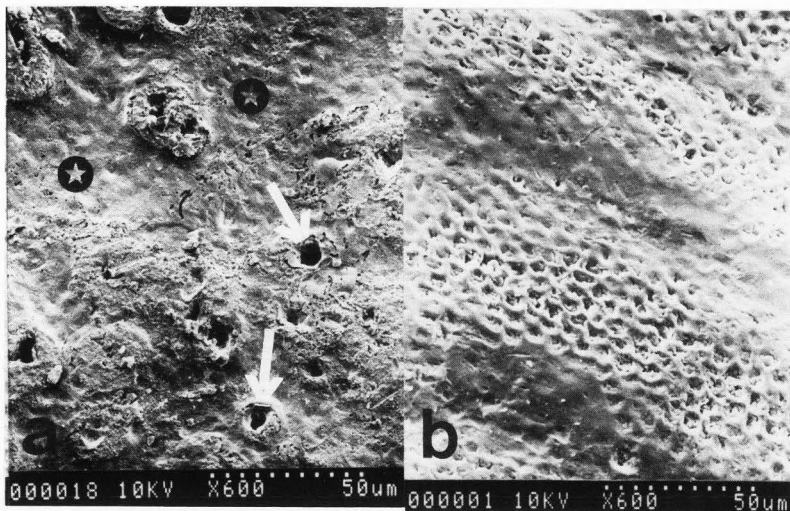


Figure 4. Scanning electron micrograph at the same magnification (bar = 100 μm) of enamel surfaces. The organic film at the surface of these two teeth have been removed by the cleaning during 5 minutes in 10% sodium hypochlorite solution. (a) Affected enamel. Note the presence of numerous 5 to 10 μm diameter pits (arrows). In some place, this enamel surface presents a prismatic structure. (b) Healthy enamel. There are no pits. Note the prismatic structure and *perikymatia*.

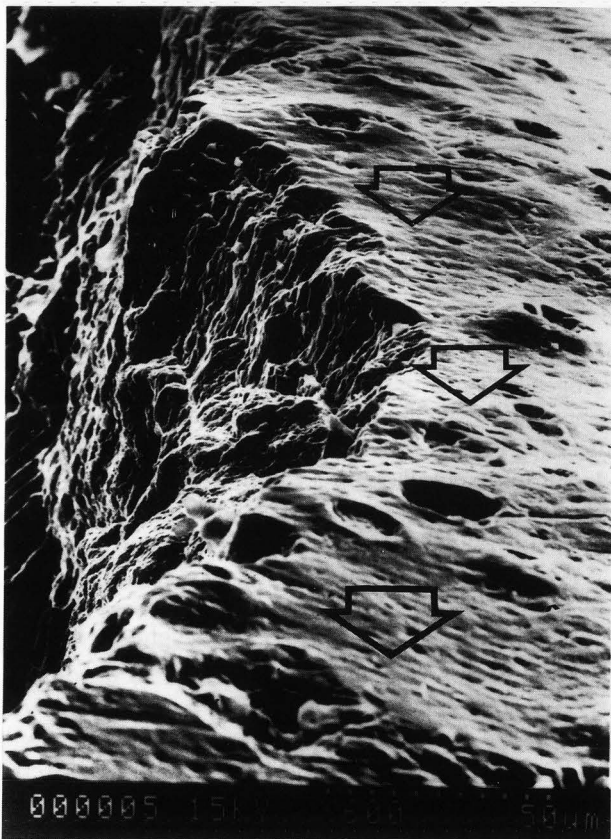


Figure 5. Scanning electron micrograph of the broken surface of affected enamel revealing a prismatic structure with pits making channels in the enamel thickness. Large arrows: enamel surface.

Powdered samples were sieved smaller than 10 μm , diluted at 2% in KBr and pelleted under 8×10^8 Pa pressure. Healthy enamel, affected enamel and affected dentin were studied using FTIRS in the transmission

mode in order to evaluate the relative variations in PO_4^{3-} , HPO_4^{2-} , CO_3^{2-} and OH^- groups in enamel and dentin. The spectra were obtained using a Bruker IFS 88 spectrophotometer in the 400–4000 cm^{-1} region. The FTIR contributions of atmospheric CO_2 and water were subtracted using the spectrum of a pure KBr pellet.

The XRD patterns of the powdered enamel were obtained in the 4–30° range with $\text{CuK}\alpha_1$ radiation (0.15406 nm), using a Jobin Yvon Sigma 2080 Spectrophotometer, working by reflection and operating at 40 kV, 25 mA.

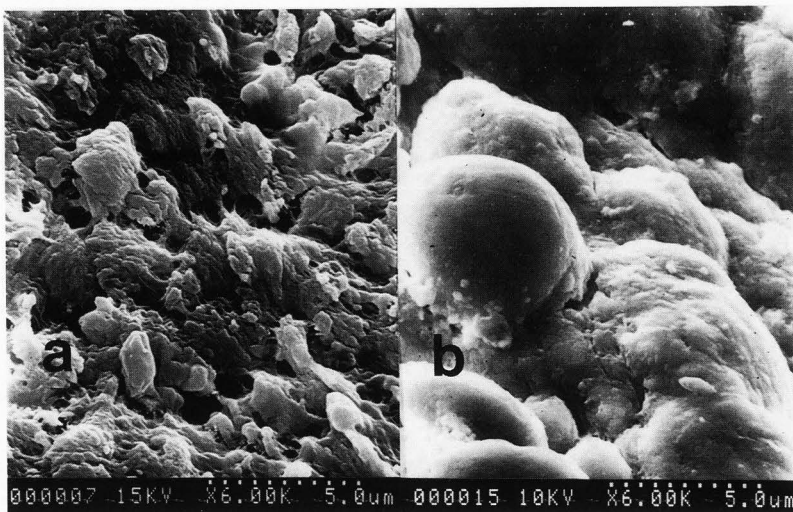
As these fourteen teeth were harvested from the same patient, statistical analysis was considered to be of no significance.

Results

SEM examination of the polished sections of premolars (Fig. 2) showed on backscattered electron images that the enamel thickness varied from the occlusal to the buccal surface between 450 and 1050 μm instead of about 2500 μm in the buccal area of healthy enamel. An heterogeneous area of lower density involving the inner first third appeared close to the dentino-enamel junction (DEJ). Some cracks seemed to correlate with weakness lines but most of them were artifacts. No tufts or enamel spindles were observed. At a higher magnification (Fig. 3), the area adjacent to the dentino-enamel junction revealed a very thin aprismatic area and a thick porous zone where prism sheath and interprismatic substance were enlarged in the first inner 100–150 μm .

The examination of affected enamel surfaces (Fig. 4a) revealed the presence of numerous irregularly distributed pits with diameters of about 5 to 10 μm . The control healthy enamel surface did not present any pits but a superficial prismatic structure between *perikymatia* (Fig. 4b).

Figure 6. Scanning electron micrograph of two teeth: one affected bicuspid (a) and one control bicuspid (b). Each of these observed areas are located in the middle third of the roots. (a) Affected cementum. Small uncoalesced aggregates of crystallites. (b) Normal aspect of sound cementum at the same magnification (bars = 10 μm).



On the broken part of affected enamel (Fig. 5), pits observed on the surface corresponded to channels which were opened by the fracture. This view did not allow for measurement of their length; however, these channels could be associated with the untimely death of ameloblasts. On the fractured line, the modifications of the enamel rod orientation and the coincidence with a *perikymatia* could be a *stria* of Retzius.

Examination of the external part of the roots of two teeth (one affected bicuspid and one control bicuspid, Fig. 6) revealed either strongly modified cementum or a total lack of this tissue, leaving the dentin visible. Where present, cementum was made up of small uncoalesced aggregates of crystallites between which some opened dentinal tubules were seen (Fig. 6a). This flattened structure differed strongly from the appearance of normal cementum (Fig. 6b).

When cementum was missing (Fig. 7), the outer radicular dentin surface showed numerous resorption *lacunæ* of various size and configuration leaving some characteristic dentinal tubules visible.

Examination of the upper right lateral permanent incisor root (Fig. 8) revealed an unusual appearance of the dentin due to its replacement by osseous tissue. Some opened tubules allowed the identification of the remaining dentin.

The X-ray diffractogram of altered enamel (Fig. 9a) showed the main reflections of apatite mineral. In comparison with a healthy enamel apatite (Fig. 9b), the structure was disordered, as revealed by the low intensities and broadenings of reflection-peaks. There was also a reflection near 0.292 nm (* at 15.30° θ) that did not belong to the set of apatite peaks. This may be the main peak of tricalcium phosphate, $\text{Ca}_3(\text{PO}_4)_2$ (Powder Diffraction File, 1990).

SIMS revealed that the Ca concentrations were

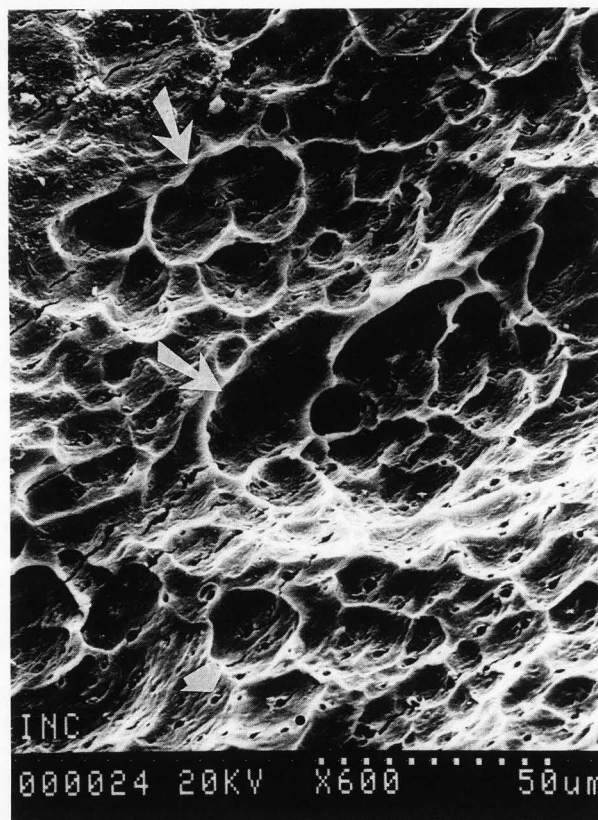


Figure 7. Examination of a root surface without cementum revealing an irregular external resorption area with numerous resorption *lacunæ* (long arrows). Note the presence of some characteristic dentinal tubules (short arrow).

between 40.2 ± 0.4 and 43.4 ± 0.4 weight % (wt%) (Table 2). These Ca concentrations were higher in altered enamel than in healthy enamel: Ca = 40.5 wt% instead of 37.8 wt% (Table 3) and uniform 40.2 to 41

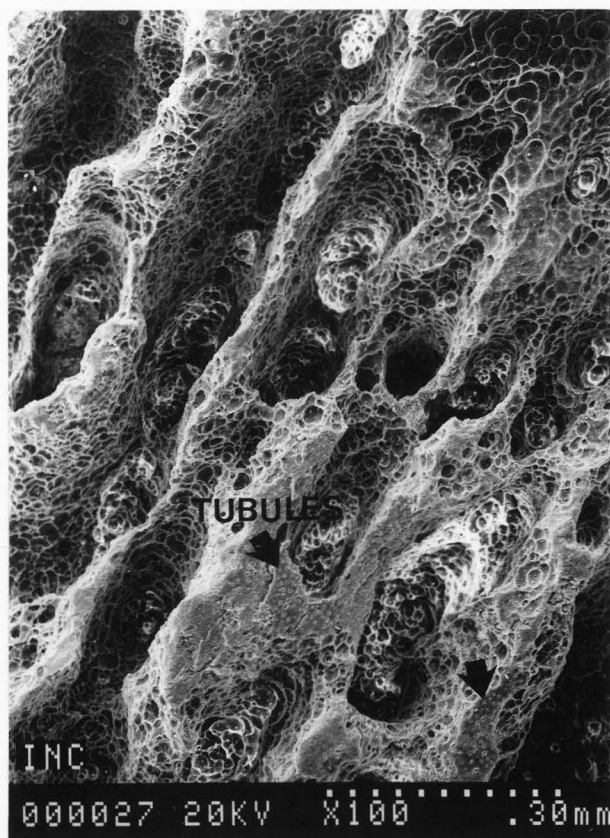


Figure 8. Examination of the upper right lateral permanent incisor root revealing an unusual appearance of the stripped dentin due to its replacement by osseous tissue. Opened dentinal tubules in limited areas (arrows) allowed the identification of the observed structure as a resorbed dentin. Bar = 100 μ m.

wt% throughout the whole enamel (Fig. 10b). Ca values were higher and much more variable in the dentin (40.5 to 43 wt%). In comparison with healthy dentin (Table 3), Ca is more concentrated in this altered dentin. The P contents were close to normal in the altered enamel (Table 2), but slightly less variable (17.4 to 18) than the Ca contents. These P values decreased from 18.0 ± 0.1 wt% in the subsurface enamel to 17.4 ± 0.1 wt% in the inner enamel. The P concentration decreased in the dentin and was lower than the normal teeth (Table 3). The Ca/P weight ratios were 2.28 in the altered enamel and 2.65 in the altered dentin, these values were higher than the average weight values for healthy enamel and dentin (about 2.10 and 2.08, respectively). The Na, Mg and F contents (Fig. 10c) were normal or close to normal.

The IR absorption spectra of the enamel and dentin (Fig. 11a) were closely similar. The O-H stretching vibrations of hydrogen-bonded water were observed at 3365 cm^{-1} . The structural OH stretching vibrations at

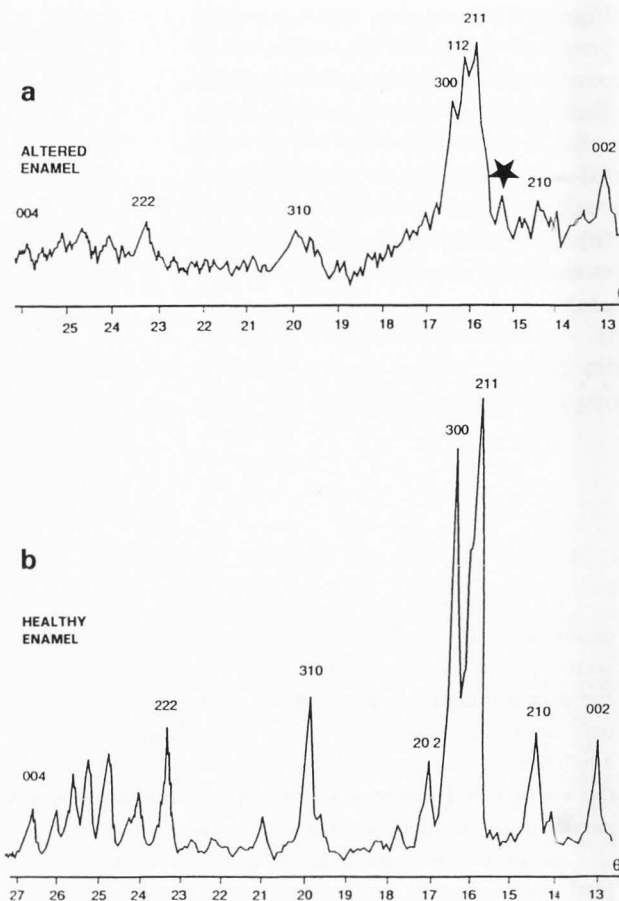


Figure 9. X-ray diffractogram of altered enamel (a) compared to that of sound enamel (b). Note the loss of intensity of the main reflections of apatite mineral and a characteristic tricalcium phosphate peak *. The spectra are indexed according to Miller's nomenclature of apatite planes as indicated by Kay *et al.* (1964).

3570 cm^{-1} , which are characteristic of healthy enamel (Driessens, 1982) or well crystallized hydroxyapatite (Cant *et al.*, 1971), were present only as a small shoulder for enamel associated with two bands at 3620 cm^{-1} and 3694 cm^{-1} .

The weakness or absence of the OH band at 3570 cm^{-1} and the presence of the amide peak at 1659 cm^{-1} , larger in affected than in healthy enamel, allowed the superimposition of the affected enamel and dentin spectra.

The presence in the overtone region of a weak band around $2100\text{--}1950 \text{ cm}^{-1}$, with a maximum at 1990 cm^{-1} , could be attributed to octocalcium phosphate (OCP) but also to hydroxyapatite (Fowler *et al.*, 1966).

The $1400\text{--}1600 \text{ cm}^{-1}$ region (Fig. 11b) assigned to CO_3^{2-} inorganic ions was partly obscured by the strong amide band from matrix protein (amide I, II and III at $1659, 1515$ and 1240 cm^{-1}).

Dental abnormalities in hyperphosphatasemia

Table 2. Experimental data on chemical characterization of enamel and dentin by SIMS.

Distance from the surface in μm	Ca wt%* ± 0.4	P wt%* ± 0.1	Ca/P
Enamel surface	41.0	17.6	2.3
70	40.6	17.6	2.3
140	40.4	18.0	2.2
210	40.8	17.7	2.3
280	40.5	17.9	2.2
350	40.4	18.0	2.2
420	40.5	17.8	2.3
490	40.4	17.9	2.2
560	40.4	17.9	2.2
630	40.5	17.8	2.3
700	40.5	17.7	2.3
770	40.5	17.7	2.3
840	40.4	17.7	2.3
910	40.3	17.7	2.3
980	40.4	17.7	2.3
1050	40.2	17.7	2.3
1120	40.3	17.7	2.3
1191	40.6	17.4	2.3
Enamel	40.4	17.6	2.3
DEJ			
dentin			
1330	42.8	16.0	2.7
1400	40.5	17.5	2.3
1410	43.4	15.6	2.8
1540	43.0	15.7	2.7
1610	42.9	15.9	2.7

*Ca and P percent weight distribution was determined along a line from the enamel surface toward the dentin of the sectioned sample (Fig. 10a) using the step scan mode. The accuracy of the SIMS was 1%.

The peaks at 1545 and 1420 cm^{-1} , associated with the broad and asymmetric bands characteristic of a doublet with a maximum at 875 cm^{-1} , (detected in the 850-900 cm^{-1} region), seemed to reveal the carbonate in the hydroxyl (type A) and phosphate (type B) sites of the apatite framework.

Discussion

The relationship between hyperphosphatasemia and dental disorders is not well established. Stemmermann (1966), Eyring and Eisenberg (1968), and Caffey (1973), have previously suggested that hyperphosphatasemia disorders were not entirely limited to bone, as skin, eyes, ears, the cardiorespiratory system, and teeth

Table 3. Experimental and published data. The mean Ca and P values and Ca/P ratio of tooth enamel and dentin affected by hyperphosphatasemia.

Experimental Data			
	Ca wt% mean \pm SD	P wt% mean \pm SD	Ca/P mean
Enamel	40.5 \pm 0.13	17.7 \pm 0.12	2.28
Dentin	42.5 \pm 1.03	16.0 \pm 0.69	2.65
Published data			
	Ca wt% normal values	P wt% normal values	Ca/P normal
Healthy human enamel (LeGeros)	37.8	18.0	2.10
Healthy human dentin (LeGeros)	36.1	17.3	2.08
Durango apatite (Roeder)	38.6	17.9	2.15

The experimental values for hyperphosphatasemia should be compared with the mean values obtained from healthy human enamel and dentin by LeGeros (1991), and from Durango apatite by Roeder *et al.* (1987). Healthy enamel and dentin are Ca deficient in comparison with Durango apatite (Table 1). In contrast, hyperphosphatasemic enamel and dentin were Ca-rich. SD = standard deviation.

may be involved. Nevertheless, Caffey's definition of this disease due to increased bone turnover did not include the modifications of enamel or dentin. It is therefore difficult to include all the dental anomalies observed here in the definition of hyperphosphatasemia.

The term *amelogenesis imperfecta* has been defined to include a variety of genetically determined disorders affecting only the enamel of all, or nearly all, teeth without detectable alterations elsewhere in the body (Witkop, 1989). Alteration of enamel formation by hyperphosphatasemia only occurs during amelogenesis. Since the enamel anomalies observed here are associated with other dentin and bone disorders, they cannot be amelogenesis imperfecta.

As most of the hyperphosphatasemia descriptions concern children, it was difficult, except in the cases of untimely loss of teeth, to determine if resorption of the deciduous teeth was pathological or not. Moreover, even when dental problems were not emphasized in papers about hyperphosphatasemia, careful examination

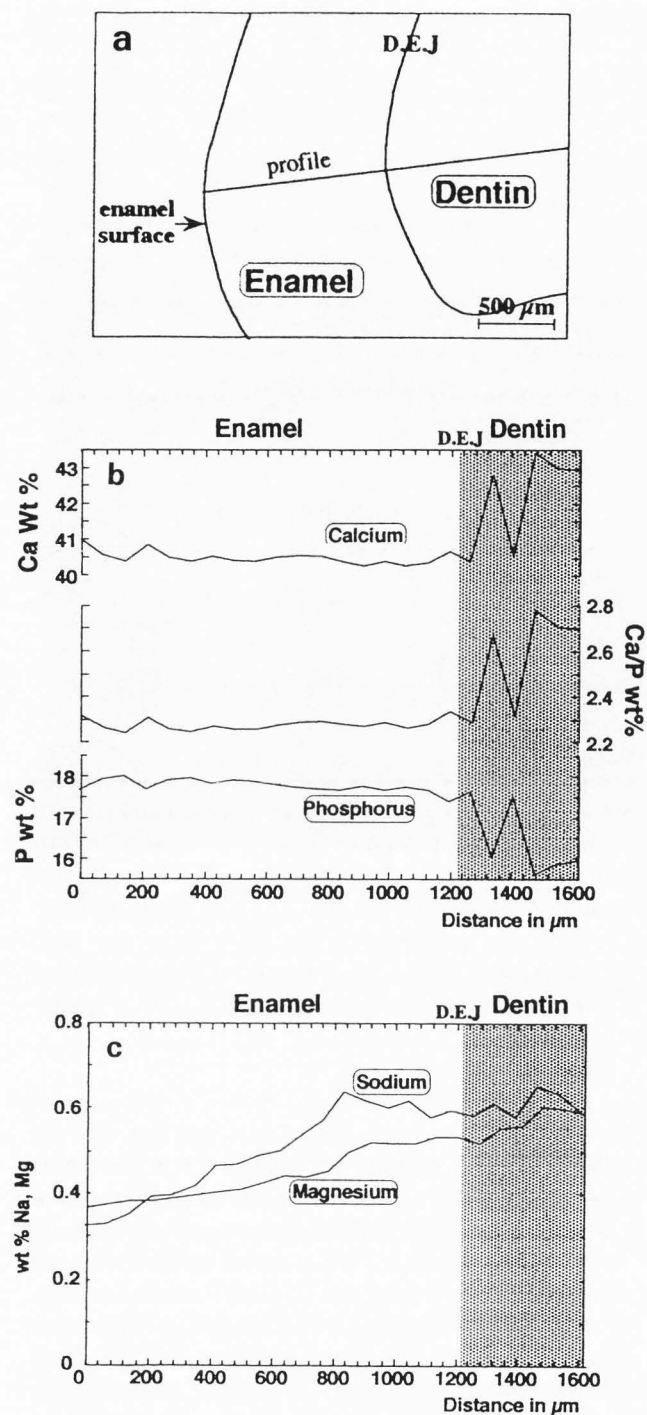


Figure 10 (a). Ca and P wt% distribution has been determined along a line from the enamel surface toward the dentin of the sectioned sample using the step scan mode. **(b)** Distribution profiles of Ca, P, obtained by SIMS revealing the high Ca concentrations ($> 40.2\%$) and the high Ca/P weight ratios ($2.2 < \text{Ca/P} < 2.8$) both in enamel and dentin. **(c)** Distribution profiles of Na and Mg. Note the normal Na and Mg concentrations.

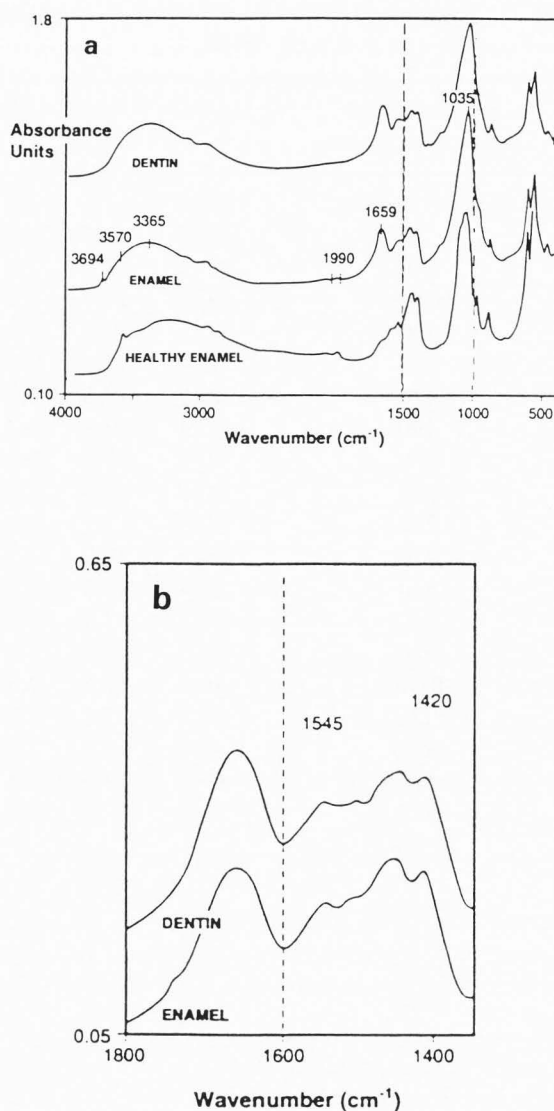


Figure 11 (a). IR Fourier-transform spectra obtained in transmission mode in healthy enamel (1), altered enamel (2), and altered dentin (3), revealing the loss of the O-H stretching vibration of hydrogen-bonded water band at 3570 cm^{-1} and therefore, a great similarity between the spectra of both altered enamel and dentin (spectra 1 and 2). **(b)** The $1400\text{--}1800 \text{ cm}^{-1}$ region assigned to the amide from matrix protein and to CO_3^{2-} inorganic ions, reveals the carbonate in the two sites of the apatite framework.

of published radiographs (Fanconi *et al.*, 1964; Bakwin *et al.*, 1964; Döhler *et al.*, 1986; Nerlich *et al.*, 1992) revealed dental lesions that could have been pointed out if the authors' concern had been dental pathology. In the present case, the patient being an adult, the lesions of the roots were undoubtedly pathological resorption.

The multimethodological analysis of the mineral phase of enamel and dentin revealed 5 particularities:

[1] IR spectra of enamel and dentin were unusually similar and revealed some features distinct from those of pure Ca(OH)-apatites reported by Fowler (1974) or of mature materials reported by Aoba and Moreno (1990).

[2] The participation of magnesium is of particular interest. As revealed by the additional OH band at 3694 cm^{-1} , that may be assigned to OH stretching vibrations of magnesium hydroxide (Farmer, 1974) or to Mg adsorbed onto apatite (Ishikawa *et al.*, 1989, 1991; Spencer *et al.*, 1989; Aoba *et al.*, 1992a,b; Bigi *et al.*, 1992; Tung *et al.*, 1992), Mg^{2+} ions could be present either in a distinct $\text{Mg}(\text{OH})_2$ phase or in an hydroxylated Mg adsorbed onto the apatite phase. Nevertheless, the SIMS data showed that the Mg concentrations and spatial distribution are essentially the same as those in healthy teeth. Thus, the hydroxylated Mg is more likely to be evenly distributed over the phosphate mineral surfaces, than to form a distinct $\text{Mg}(\text{OH})_2$ phase, which could be revealed by local clusters. This is corroborated by recent studies (Aoba *et al.*, 1992a,b; Bigi *et al.*, 1992, 1993; Tung *et al.*, 1992) showing that part of the Mg pool in the mineral phase of teeth could be adsorbed onto the apatite crystal surfaces. Bound to OH groups or adsorbed onto the mineral surfaces, Mg^{2+} ions have been shown to be directly associated with inhibition of phosphate growth and poor crystal development in enamel and dentin.

[3] The high Ca concentrations and the change in the Ca/P ratios measured by SIMS were very different from those measured in the normal teeth. In this case, the Ca/P unusually increased from the surface toward the dentino-enamel junction and then into the dentin. These high Ca concentrations can neither be explained by the presence of α TCP (tricalcium phosphate), nor by the participation of inorganic CO_3^{2-} because the relative concentration of these CO_3^{2-} ions, calculated by comparing with the $\nu_4\text{PO}_4$ band, is lower in the affected enamel and dentin than in healthy enamel. Inorganic carbonate, therefore, cannot explain the high Ca concentration. Alternatively, protein may have complexed Ca^{2+} ions and increased its relative concentration. The poor crystallinity also seems to be linked to the high content of protein revealed by the large band attributed to amide. Because of the absence of the bands at 913 or 917 cm^{-1} , more definitive for identifying OCP (octocalcium phosphate) than the 2100 - 1950 cm^{-1} bands used by Fowler *et al.* (1966, 1993), it is not possible to confirm the presence of OCP in the present samples.

[4] IR spectra revealed mineral carbonates. As in normal enamel and dentin, the peaks at 1545 - 1420 cm^{-1} and 875 cm^{-1} revealed type A and B carbonates (Emerson and Fischer, 1962; Elliott, 1965; LeGeros *et al.*,

1969; Bonel, 1972; Bonel *et al.*, 1975; Okazaki, 1983; Elliott *et al.*, 1985; LeGeros *et al.*, 1987; Rey *et al.*, 1991a,b; Sydney-Zax *et al.*, 1991). Quantitative comparison of the integrated absorbances of the band at 1545 cm^{-1} in enamel and dentin, by using the procedure of Bottero-Cornillac *et al.* (1992), showed that carbonates replace fewer OH groups in enamel than in dentin. The intensity of the band at 1420 cm^{-1} assigned to CO_3^{2-} ions replacing a PO_4^{3-} group, is higher than in the $\nu_3\text{-PO}_4$ domain. CO_3^{2-} ions are known to alter crystallinity, and increase the solubility of synthetic apatites (Elliott *et al.*, 1985; Rey *et al.*, 1991c). The synergistic effects of Mg^{2+} and Na^+ have the same result (Amjad *et al.*, 1984; Campbell *et al.*, 1991; LeGeros, 1991; Bigi *et al.*, 1992, 1993).

[5] The X-ray diffraction patterns showed that the mineral phases were poorly crystallized. A minor α -tricalcium phosphate phase (peak at 0.292 nm : $15.30^\circ \theta$) was present. The poor crystallinity of the teeth mineral phase could explain its lability and the clinical symptoms observed here. The high turnover of bone associated with hyperphosphatasemia, requires a high level of alkaline phosphatase, and a continuous and high level of mineral production. Alkaline phosphatase are involved in the transport of calcium and phosphate across cell membranes (Wöltgens *et al.*, 1982), and in the mineralization processes of root cementum (Beertsen and Van den Bos, 1989). The high alkaline phosphatase activity observed in hyperphosphatasemia, may be associated with general phosphate metabolism and periodontium remodeling, as described by Groeneveld *et al.* (1993), in the periodontal ligament of the continuously growing rat incisor.

The numerous aggregates of crystallites making up the affected cementum, and the modifications of the dentin may be the occurrence of the accelerated mineralization of the periodontium associated with a rapid remodeling affecting both cementum and dentin.

Therefore, hyperphosphatasemia appears to be consistently associated with the dental abnormalities described above.

The early diagnosis of a mild form of hyperphosphatasemia could, therefore, be based on the analysis of its dental manifestations when dental abnormalities can be clinically observed before the systemic manifestations of the disease become obvious.

Acknowledgements

We wish to thank J.P. Proust, Professor and Research Director, Laboratory IMEB (Biomaterial/extracellular matrix interface), Université de la Méditerranée, for his helpful assistance in rewriting this paper.

References

- Amjad Z, Koutsoukos PG, Nancollas GH. (1984). The crystallization of hydroxyapatite and fluoroapatite in the presence of magnesium ions. *J. Colloid. Interf. Sci.* **101**: 250-256.
- Aoba T, Moreno EC. (1990). Changes in the nature and composition of enamel mineral during porcine amelogenesis. *Calcif. Tissue Int.* **47**: 356-364.
- Aoba T, Moreno EC, Shimoda S. (1992a). Competitive adsorption of magnesium and calcium ions onto synthetic and biological apatites. *Calcif. Tissue Int.* **51**: 143-150.
- Aoba T, Shimoda S, Moreno EC. (1992b). Labile of surface pools of magnesium, sodium, and potassium in developing porcine enamel mineral. *J. Dent. Res.* **71**: 1826-1831.
- Bakwin H, Eiger MS. (1956). Fragile bones with macrocranium. *J. Pediatr.* **49**: 558-564.
- Bakwin H, Golden A, Fox S. (1964). Familial osteoectasia with macrocranium. *Am. J. Roentgenol.* **91**: 609-617.
- Beertsen W, Van den Bos T. (1989). Calcification of dentinal collagen by cultured rabbit periosteum: the role of alkaline phosphatase. *Matrix* **9**: 159-171.
- Bigi A, Foresti E, Gregorini R, Ripamonti A, Roverti N, Shah JS. (1992). The role of magnesium on the structure of biological apatites. *Calcif. Tissue Int.* **50**: 439-444.
- Bigi A, Falini G, Foreti E, Gazzano M, Ripamonti A, Roveri N. (1993). Magnesium influence on hydroxyapatite crystallization. *J. Inorg. Biochem.* **49**: 69-78.
- Bonel G. (1972). Contribution à l'étude de la carbonatation des apatites (Contribution to the study of the incorporation of carbonate in apatites). *Ann. Chim.* **7**: 65-88.
- Bonel G, Labarthe JC, Vignoles C. (1975). Contribution à l'étude structurale des apatites carbonatées de type B (Contribution to the structural study of type B carbonate apatites). *Coll. Int. CNRS, Editions CNRS, (Paris)* **230**: 117-125.
- Bottero-Cornillac MJ, Yvon J, Vadot J. (1992). Multimethod analysis of apatites in sound human tooth enamel. *Eur. J. Mineral.* **4**: 1347-1357.
- Caffey J. (1973). Familial hyperphosphatasemia with ateliosis and hypermetabolism of growing membranous bone; review of the clinical, radiographic and chemical features. In: *Progress in Pediatric Radiology: Vol. 4: Intrinsic Diseases of Bones.* Kaufmann HJ (ed.). Karger, Basel, Switzerland. pp. 438-468.
- Caffey J. (1977). Therapeutic value of thyrocalcitonin. *Am. J. Roentgenol.* **129**: 175-179.
- Campbell AA, Nancollas MLR, Nancollas GH. (1991). The influence of carbonate and magnesium ions on the growth of hydroxyapatite, carbonated apatite and human powdered enamel. *Colloid Surface.* **54**: 25-31.
- Cant NW, Bett JAS, Wilson GR, Hall WK. (1971). The vibrational spectrum of hydroxyl groups in hydroxyapatites. *Spectrochim. Acta* **27**: 425-439.
- Döhler JR, Souter WA, Beggs I, Smith GD. (1986). Idiopathic hyperphosphatasia with dermal pigmentation. *J. Bone Joint Surg.* **68**: 305-310.
- Diressens FCM. (1982) Mineral aspects of dentistry. In: *Monographs in Oral Science.* Vol. **10.** Myers HM (ed.). Karger, Basel. pp. 55-56.
- Dunn V, Condon VR, Rallison ML. (1979). Familial hyperphosphatasemia: Diagnosis in early infancy and response to human thyrocalcitonin therapy. *Am. J. Roentgenol.* **132**: 541-545.
- Elliott JC. (1965). The interpretation of the infrared absorption spectra of some carbonate-containing apatites. In: *Tooth Enamel.* Stack MV, Fearnhead RW (eds.). John Wright, Bristol, UK. pp. 20-22.
- Elliott JC, Holcomb DW, Young RA. (1985). Infrared determination of the degree of substitution of hydroxyl by carbonate ions in human dental enamel. *Calcif. Tissue Int.* **37**: 372-375.
- Emerson WH, Fischer ED. (1962). The infrared absorption spectra of carbonate in calcified tissues. *Arch. oral Biol.* **7**: 671-683.
- Eyring EJ, Eisenberg E. (1968). Congenital hyperphosphatasia. A clinical, pathological, and biochemical study of two cases. *J. Bone Joint Surg.* **50**: 1099-1117.
- Fanconi G, Moreira G, Uehlinger E, Giedion A. (1964). Osteochalasia desmialis familiaris; hyperostosis corticalis deformans juvenilis, chronic idiopathic hyperphosphatasia, osteoectasia and macrocranium. *Helv. Paediatr. Acta.* **19**: 279-295.
- Farmer WC. (1974). *The Infrared Spectra of Minerals.* Mineralogical Society. London. p. 390.
- Fowler BO. (1974). Infrared studies of apatites. I. Vibrational assignments for calcium, strontium, and barium hydroxyapatites utilizing isotopic substitution. *Inorg. Chem.* **13**: 194-207.
- Fowler BO, Moreno EC, Brown WE. (1966). Infrared spectra of hydroxyapatite octacalcium phosphate and pyrolysed octacalcium phosphate. *Arch. oral Biol.* **11**: 447-492.
- Fowler BO, Markovic M, Brown WE. (1993). Octacalcium phosphate. 3. Infrared and Raman vibrational spectra. *Chem. Mater.* **5**: 1417-1423.
- Groeneveld MC, Everts V, Beertsen W. (1993). A quantitative enzyme histochemical analysis of the distribution of alkaline phosphatase activity in the periodontal ligament of the rat incisor. *J. Dent. Res.* **72**: 1344-1350.
- Iancu TC, Almagor G, Friedman E, Hardoff R, Front D. (1978). Chronic familial hyperphosphatasemia. *Pediatr. Radiol.* **129**: 669-676.

Dental abnormalities in hyperphosphatasemia

- Ishikawa T, Wakamura M, Kondo S. (1989). Surface characterization of calcium hydroxyapatite by Fourier transform infrared spectroscopy. *Langmuir* **5**: 140-144.
- Ishikawa T, Wakamura M, Kawase T. (1991). Surface characterization by X-ray photoelectron spectroscopy and Fourier transform infrared spectroscopy of calcium hydroxylapatite coated with silicate ions. *Langmuir* **7**: 596-599.
- Kay MJ, Young RA, Posner AS. (1964) Crystal structure of hydroxyapatite. *Nature* **204**: 1050-1052.
- Kerebel B, Daculsi G. (1977). Ultrastructural study of amelogenesis imperfecta. *Calcif. Tissue Res.* **24**: 191-197.
- LeGeros RZ. (1991). Calcium phosphates in oral biology and medicine. In: *Monographs in Oral Science*. Vol. 15. Myers HM. (ed.). Karger, Basel. pp. 108-129.
- LeGeros RZ, Trautz OR, Klein E, LeGeros JP. (1969). Two types of carbonate substitution in the apatite structure. *Experientia* **25**: 5-7.
- LeGeros RZ, Abergas T, Blednas H, LeGeros JP. (1987). CO₃-for-OH (type A) and CO₃-for-PO₄ (type B) substitutions in precipitated carbonate-apatites. *J. Dent. Res.* **66**: 667 (abstract).
- Nerlich AG, Brenner RE, Müller PK, Remberger K. (1992). Multifocal osteogenic sarcoma of the skull in a patient who had congenital hyperphosphatasemic skeletal dysplasia. *J. Bone Joint Surg.* **74**: 1090-1095.
- Okazaki M. (1983). F⁻-CO₃²⁻ Interaction in IR spectra of fluoridated CO₃-apatites. *Calcif. Tissue Int.* **35**: 78-81.
- Powder Diffraction File. (1990). International Center for Diffraction Data Publications. (Joint Committee on Powder Diffraction Standards) *JCPDS* 9-348; 29-359.
- Rey C, Renugopalakrishnan V, Collins B, Glimcher MJ. (1991a). Fourier transform infrared spectroscopic study of the carbonate ions in bone mineral during aging. *Calcif. Tissue Int.* **49**: 251-258.
- Rey C, Renugopalakrishnan V, Shimizu M, Collins B, Glimcher MJ. (1991b). A resolution-enhanced Fourier transform infrared spectroscopic study of the environment of the CO₃²⁻ ion in the mineral phase of enamel during its formation and maturation. *Calcif. Tissue Int.* **49**: 259-268.
- Rey C, Shimizu M, Collins B, Glimcher MJ. (1991c). Resolution-enhanced Fourier transform infrared spectroscopy study of the environment of phosphate ions in the early deposits of a solid phase of calcium-phosphate in bone and enamel, and their evolution with age. 2. Investigations in the n₃PO₄ domain. *Calcif. Tissue Int.* **49**: 383-388.
- Roeder PL, MacArthur D, Ma XP, Palmer GR, Mariano AN. (1987). Cathodoluminescence and microprobe study of rare-earth elements in apatite. *Am. Mineralogist* **72**: 801-811.
- Spencer P, Barnes C, Martini J, Garcia R, Elliott C, Doremus R. (1989). Incorporation of magnesium into rat dental enamel and its influence on crystallization. *Arch. oral Biol.* **34**: 767-771.
- Spindler A, Berman A, Mautalen C, Ubios J, Santini E. (1992). Chronic idiopathic hyperphosphatasia. Report of a case treated with pamidronate and a review of the literature. *J. Rheumatol.* **19**: 642-645.
- Stemmermann GN. (1966). An histologic and histochemical study on familial osteoectasia (Chronic Idiopathic Hyperphosphatasia). *Am. J. Pathol.* **48**: 641-651.
- Sydney-Zax M, Mayer I, Deutsch D. (1991). Carbonate content in developing human and bovine enamel. *J. Dent. Res.* **5**: 913-916.
- Thompson RC, Gaull GE, Horwitz SJ, Schenk RK. (1969). Hereditary hyperphosphatasia. *Am. J. Med.* **47**: 209-219.
- Tung MS, Tomazic B, Brown WE. (1992). The effects of magnesium and fluoride on the hydrolysis of octacalcium phosphate. *Arch. oral Biol.* **37**: 585-591.
- Whalen JP, Horwith M, Krook L, Mac Intyre I, Mena E, Viteri F, Torun B, Nunez EA. (1977). Calcitonin treatment in hereditary bone dysplasia with hyperphosphatasemia: A radiographic and histologic study of bone. *Am. J. Roentgenol.* **129**: 29-35.
- Witkop CJ Jr. (1989). Amelogenesis imperfecta, dentinogenesis imperfecta and dentin dysplasia revisited: Problems in classification. *J. Oral Pathol.* **17**: 547-553.
- Wöltgens JHM, Bervoets TJM, Bronckers ALJJ, Lyaruu DM. (1982). Organ culture of tooth germs: Relationship between alkaline phosphatase and mineralization *in vitro*. *J. Biol. Buccale* **10**: 191-198.

Discussion with Reviewers

T. Aoba: Inconsistently, FTIR exhibited the amide band derived from the organic matter. Please comment.
Authors: As stated in the text, because of the relatively short period during which NaOCl was used and its relatively low concentration (according to the procedure of Kerebel and Daculsi, 1977), only the organic film at the surface of teeth was removed. The internal organic matter was not removed, and therefore, the FTIR spectra exhibit the amide band derived from this organic component.

T. Aoba: It is most unlikely that relatively low amounts of Mg on apatite surfaces yield effects on FTIR spectra. Please comment.

Authors: Because of the very high molar extinction coefficient of OH in IR spectroscopy, low quantities of adsorbed OH on the apatite surface give rise to a signal

(Ishikawa *et al.*, 1989). The IR band at 3694 cm^{-1} can be assigned to OH stretching vibrations and Farmer (1974) showed that OH bound to Mg^{2+} cations is responsible for this signal. According to our observations, the concentration of Mg^{2+} is about $0.5\% \pm 0.1\%$ (see Fig. 10). According to Ishikawa *et al.* (1989) and Farmer (1974), these quantities are sufficient to result in some effect on the FTIR spectra.

M. Goldberg: Regarding Figure 7, Boyde has previously reported that during dentin resorption differences appear in the destruction pattern between peritubular and intertubular dentin. Did the authors obtain some evidence of that?

Authors: In Figure 7, it appears that the peritubular and the intertubular dentin undergo simultaneous destruction.